Article

N- and O-Glycosylation of the SARS-CoV-2 Spike Protein

Miloslav Sanda,* Lindsay Morrison, and Radoslav Goldman

Cite This: https://dx.doi.org/10.1021/acs.analchem.0c03173

Read Online

ACCESS | Metrics & More | Article Recommendations | Supporting Information

ABSTRACT: Covid-19 pandemic outbreak is the reason of the current world health crisis. The development of effective antiviral compounds and vaccines requires detailed descriptive studies of SARS-CoV-2 proteins. The SARS-CoV-2 spike (S) protein mediates virion binding to the human cells through its interaction with the ACE2 cell surface receptor and is one of the prime immunization targets. A functional virion is composed of three S1 and three S2 subunits created by furin cleavage of the spike protein at R682, a polybasic cleavage site that differs from the SARS-CoV spike protein of 2002. By analysis of the protein produced in HEK293 cells, we observe that the spike is O-glycosylated on a threonine (T678) near the furin cleavage site occupied by core-1 and core-2 structures. In addition, we have identified eight additional O-glycopeptides on the spike glycoprotein and confirmed that the spike protein is heavily N-glycosylated. Our recently developed liquid chromatography—mass spectrometry methodology allowed us to identify LacdiNAc structural motifs on all occupied N-glycopeptides and polyLacNAc structures on six glycopeptides of the spike protein. In conclusion, our study substantially expands the current knowledge of the spike protein's glycosylation and enables the investigation of the influence of O-glycosylation on its proteolytic activation.
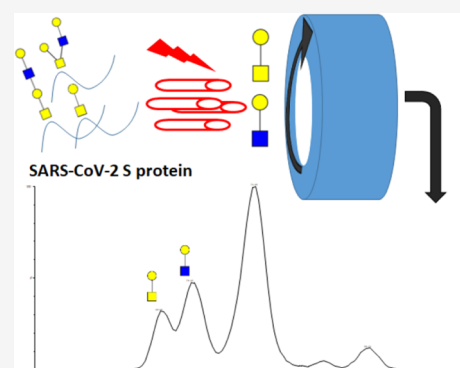
INTRODUCTION

The World Health Organization was informed of pneumonia cases of unknown etiology in Wuhan, Hubei Province, China, on 31 December 2019.[1] A novel coronavirus was identified as the cause of the disease by further investigations.[2] This new virus is related to the previously identified SARS-CoV (severe acute respiratory syndrome coronavirus) and has been named SARS-CoV-2 (severe acute respiratory syndrome coronavirus 2). Symptoms of the coronavirus disease 2019 (COVID-19) are acute onset of fever, myalgia, dyspnea, cough, and evidence of ground-glass lung opacities. Currently, we do not have an effective vaccine or treatment for COVID-19 patients and continued research is urgently needed to address the challenges posed by the pandemic.

Transmembrane spike (S) glycoprotein of SARS-CoV-2 interacts with the angiotensin-converting enzyme 2 (ACE2) presented on the surface of human cells and mediates viral entry.[3−5] Both the viral spike and human ACE2 are glycoproteins and their glycosylation affects their interactions or vaccine design. Covid 19 spike glycoprotein forms a trimeric structure on the surface of the virus envelope 6. Each spike protein consists of an S1 and an S2 subunit; the S1 subunit mediates binding of the virus to the ACE2 receptor, while the S2 subunit enables fusion of the virion with the cell membrane and initiates viral entry. SARS-CoV-2 has 10 to 20 times higher affinity for the ACE2 receptor than the SARS-CoV[3] which may be, in part, related to glycosylation of proteins. The SARS-CoV-2 S glycoprotein carries 22 N-glycosylation sequons[6] and at least 3 sites of mucin-type O-glycosylation were predicted[7]

but were not yet observed experimentally. The latest analysis shows that 20 out of the 22 N-glycosylation sequons are occupied by complex, hybrid, and oligomannosidic structures. Some of the sequons are predominantly occupied by oligomannose structures, which could have influence on the trimeric structure. The studies also detected one O-glycopeptide occupied at sites, distinct from the predicted furin cleavage site at the S1/S2 boundary.[6,8,9]

In this study, we report the analysis of the site-specific glycoforms with focus on the resolution of structural motifs of the identified O- and N- glycopeptides. To this end, we used high-resolution liquid chromatography—mass spectrometry (LC−MS/MS) with higher energy collisional dissociation (HCD) fragmentation and modulated normalized collision energy (NCE)[10] to study a recombinant SARS-CoV-2 S full-length protein expressed in human embryonic kidney (HEK 293) cells. Our analyses identified 9 occupied O-glycopeptides and 17 N-glycopeptides. We resolved, for the first time, LacdiNAc and polyLacNAc structural motifs associated with the N-glycopeptides and identified novel O-glycopeptides including a glycopeptide near the furin cleavage site of the spike glycoprotein.

Table 1. N-Glycosylation of the SARS-CoV-2S Glycoprotein: A, LacdiNAc; B, PolyLacNAc; C, Outer Arm Fucosylation; and D, Core Fucosylation

annotated sequence	occupied site	site occupancy	identified structures	identified structural motifs
[R].SSVLHSTQDLFLPFFSNVTWFHAIHVSGTNGTK.[R]	61,74		"11"	A, C, D
[K].TQSLLIVNNATNVVIK.[V]	122	100%	63	A, C, D
[K].VCEFQFCNDPFLGVYYHKNNK.[S]	149	100%	60	A, C, D
[R].VYSSANNCTFEYVSQPFLMDLEGK.[Q]	165	100%	63	A, C, D
[R].DLPQGFSALEPLVDLPIGINITR.[F]	234	>99%	45	A, C, D
[K].YNENGTITDAVDCALDPLSETK.[C]	282	100%	62	A, B, C, D
[R].FPNITNLCPFGE.[V]	331	>99%	51	A, C, D
[E].VFNATR.[F]	344	100%	48	A, C, D
[D].VNCTEVPVAIHADQLTPTWR.[V]	616	>99%	3	A
[R].AGCLIGAEHVNNSYECDIPIGAGICASYQTQTNSPR.[A]	657	96%	53	A, C, D
[K].DFGGFNFSQILPDPSKPSK.[R]	801	>99%	30	A, C, D
[K].NFTTAPAICHDGK.[A]	1074	98%	21	A, B, C, D
[R].EGVFVSNGTHWFVTQR.[N]	1098	>99%	78	A, B, C, D
[D].VVIGIVNNTVYDPLQPE.[L]	1134	92%	11	A, B, C, D
[K].NHTSPD.[V]	1158	">99%"	4	A, D
[D].LGDISGINASVVNIQK.[E]	1173	57%	10	A, B, D
[K].NLNESLIDLQELGKYEQYIK.[W]	1194	98%	25	A, B, C, D

■ EXPERIMENTAL SECTION

Materials and Methods. *Materials.* The recombinant SARS-CoV-2 spike (R683A, R685A, His-tag) protein expressed in the HEK 293 cell line was obtained from ACROBiosystems (Newark, DE, USA). The purity of the purchased protein was >85%; detailed information is given in the certificate of analysis in the Supporting Information. Trypsin Gold and Glu-C, Sequencing Grade, were from Promega (Madison, WI); PNGase F, neuraminidase, and 1−3 and 1−4 β-galactosidases were from New England Biolabs (Ipswich, MA).

Glycopeptide Preparation. Aliquots of SARS-CoV-2 S protein were dissolved in 100 mM ammonium bicarbonate buffer pH 8 to a final concentration of 1 mg/mL. The protein solution was reduced with 5 mM dithiothreitol (DTT) for 60 min at 60 °C, alkylated with 15 mM iodoacetamide for 30 min in the dark, and digested with Trypsin Gold (2.5 ng/μL) at 37 °C in a Barocycler NEP2320 (Pressure BioSciences, South Easton, MA) for 1 h. GluC, PNGase F, neuraminidase, and β-galactosidase digests of tryptic peptides were obtained as described previously[11,12] with heat inactivation (99 °C for 10 min) prior to the addition of any enzyme.

Glycopeptide Analysis Using DDA Nano LC−MS/MS on the Orbitrap Fusion Lumos. Digested proteins were separated using a 120 min ACN gradient on a 250 mm × 75 μm C18 PepMap column at a flow rate of 0.3 μL/min, as described previously.[13] In brief, peptide and glycopeptide separation was achieved by a 5 min trapping/washing step using 99% solvent A (2% acetonitrile and 0.1% formic acid) at 10 μL/min, followed by a 90 min acetonitrile gradient at a flow rate of 0.3 μL/min: 0−3 min, 2% B (0.1% formic acid in ACN); 3−5 min, 2−10% B; 5−60 min, 10−45% B; 60−65 min, 45−98% B; 65−70 min, 98% B, and 70−90 min equilibration by 2% B. Glycopeptides were analyzed using an Orbitrap Fusion Lumos mass spectrometer with the electrospray ionization voltage at 3 kV and the capillary temperature at 275 °C. MS1 scans were performed over m/z 400−1800 with the wide quadrupole isolation on a resolution of 120,000 (m/z 200), the RF lens at 40%, the intensity threshold for MS2 set to 2.0×10^4, selected precursors for MS2 with charge states 3−8, and dynamic exclusion for 30 s. Data-dependent HCD tandem mass spectra

were collected with a resolution of 15,000 in the Orbitrap with fixed first masses of 110 and 4, and normalized collision energies (CEs) of 10, 20, and 35%. ETD and EThcD methods used calibrated charge-dependent parameters, and HCD supplemental activation was set to 15% NCE; we used the same chromatographic method and instrument settings for the ETD measurements as described above. Analysis was performed in duplicate.

Glycopeptide Analysis Using Cyclic Ion Mobility. LC-IM-MS/MS experiments were performed on a Waters Select Series cyclic ion mobility mass spectrometer with an ACQUITY M-class solvent system. Tryptic peptides were separated using a 75 μm × 150 mm ACQUITY BEH C18 column with a 5 cm Symmetry C18 trap. Peptides were eluted over 60 min prior to electrospray ionization and analysis in positive mode. Glycoforms of the polybasic peptide were isolated in the quadrupole and fragmented in the trap region prior to ion mobility separations. Ion mobility methods entailing five passes of the cyclic device were previously optimized for HexNAcHex and HexNAcHexNeuAc oxonium ions and were used to separate and characterize the oxonium ion fragments of the targeted glycopeptides. Traveling wave parameters within the cyclic device were kept at default values, 375 m/s and 22 V for the wave velocity and wave height, respectively. Calibration for the collisional cross section was performed under a single experimental condition for both single-pass and five-pass methods using Major Mix, with calculated uncertainties of less than 0.25 and 1%, respectively.

Data Analysis. *Glycopeptide Identification.* Byonic software 2.1 (protein metric) was used for the identification of summary formulas of glycans associated with glycopeptides (glycan database, 280 entries; precursor mass tolerance, 20 ppm; fragment mass tolerance, 20 ppm; maximum missed cleavages, 2; and cysteine carbamidomethylation and methionine oxidation). Independent searches were performed on data with different CE settings. All spectra of the identified glycopeptides were checked manually for the presence of structure-specific fragments. Analysis of the ion mobility data was performed using DriftScope (v2.9) by manual extraction of retention ranges associated with glycopeptides.

RESULTS AND DISCUSSION

N-Glycopeptide Analysis. We have identified 17 tryptic N-glycopeptides of the SARS-CoV-2 spike protein occupied by high mannose, hybrid, and complex glycans. We have determined their site occupancy by PNGaseF deglycosylation in [18]O water as described,[11] and we find majority of the sequons fully occupied (Table 1). We have found that one sequon is not glycosylated (N603) and that N234 is almost exclusively occupied by high mannose glycans. We do not have evidence for the occupancy of glycosite N17. The remaining 17 sequons are dominated by complex glycans (Table 1).

Structural Motifs of the N-Glycans Using Modulated CE. We used our recently described workflows, using modulation of CE for selective fragmentation of the glycopeptides,[10] to identify structural motifs of the N-glycosylated peptides of the SARS-CoV-2 S protein. We identified the LacdiNAc structural motif on all the occupied sequons of SARS-CoV-2 S expressed in HEK293 cells (Table 1). The low CE tandem mass spectrum (Figure 1) reveals
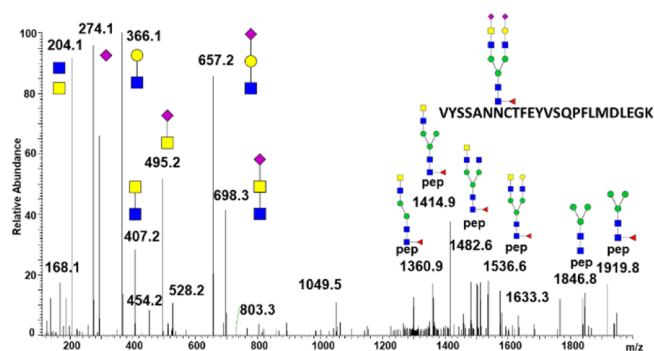

Figure 1. HCD fragmentation of the N165 glycopeptide carrying an asymmetric biantennary glycan with a sialylated LacdiNAc structural motif.

structural features of an asymmetric LacdiNAc motif contained within a disialylated biantennary N-glycan. The presence of m/z 366/407 ions distinguishes the LacNAc and LacdiNAc motifs; in addition, we observe the m/z 657/698 ions of their sialylated counterparts. In addition to the fucosylated and/or sialylated LacdiNAc, we also identified polyLacNAc structures on five N-glycopeptides (Table 1) and resolved extensive fucosylation of the core as well as the outer arms of the N-glycopeptides, as described previously.[10] The presence of core fucose on 15 sequons and the presence of outer arm fucosylation[11,14] on 7 sequons were confirmed, which are in contrast to the previously published data.[8] This might be a result of slight differences in the HEK293 expression systems

used or differences in the analytical methods. For example, our study analyzed a modified full-length protein not cleaved by convertases, which could potentially cause some differences. It is, however, more likely that the energy optimized workflows improve the structural resolution. We do not achieve complete assignment of all linkages or quantification of isobaric structures, but the presence of these structural motifs, frequently associated with specific biological functions, is clearly established. The overall results show that five glycopeptides carry polyLacNac motifs, that all sequons occupied by complex glycans carry LacdiNAc to some degree, and that the LacdiNAc structures constitute the majority (>50%) of glycoforms on N165 and N1098. It is, however, important to note that glycoforms of the spike protein will depend on the expression system used and may not necessarily reflect the glycoforms of the vition.

O-Glycopeptide Analysis. Previously published data describe one O-glycopeptide occupied at S323 and T325.[6,8] The published data were obtained by LC−MS/MS analysis of the spike protein expressed in HEK293 cells using Orbitrap-based mass spectrometers and HCD/EThcD fragmentation. We identified the same O-glycopeptides but, in addition, we have identified eight O-glycopeptides occupied by core-1 and core-2 structures (Table 2 and Table S1). Occupancy of the sites varies from <1 to 57% and is very low for at least three of the glycopeptides. However, we detect approximately 13% occupancy with core-1 and core-2 structures at T678 (Figures 2 and 3) located near the polybasic furin cleavage site between the S1 and S2 subunits, which evolved in the SARS-CoV-2 S protein.[7] Figure S1 documents the identification of an O-glycopeptide following deglycosylation with PNGaseF. This is interesting because O-glycosylation in such a close proximity to N-glycosylation is rarely described; we do not know if this has any functional relevance, but it shows that analysis of N-deglycosylated peptides for O-glycoforms may deserve attention. Retention times of T687 O-glycoforms (Figure 4) follow the expected trends of structure-dependent reverse phase chromatographic behavior of glycopeptides.[16,17]

Determination of Sites of O-Glycosylation Using EThcD. Exoglycosidase digestion and EThcD fragmentation were used to determine the exact sites occupied by glycans. We have identified nine O-glycopeptides occupied by O-glycans (Table 2). Figure 3 shows a typical ETD/EThcD fragmentation spectrum of an O-glycopeptide in this case simplified by nonspecific neuraminidase. The fragmentation shows that T687 is the major occupied site as the z6 carries a glycan but the z4 does not; the peptide is occupied by core-1 (Figure 3A) as well as core-2 (Figure 3B) structures. In addition, we used a combination of neuraminidase and $\beta1-3$ and $\beta1-4$

Table 2. O-Glycosylation of the SARS-CoV-2 S glycoprotein on Glycosite T678

| peptide	modification	%
[E].CDIPIGAGICASYQTQTNSPR.[A]	2× carbamidomethyl [C1; C10]; 1× NeuAc(2)Hex(2)HexNAc(2)	5.03
[E].CDIPIGAGICASYQTQTNSPR.[A]	2× carbamidomethyl [C1; C10]; 1× NeuAc(1)Hex(1)HexNAc(2)	0.49
[E].CDIPIGAGICASYQTQTNSPR.[A]	2× carbamidomethyl [C1; C10]; 1× Hex(2)HexNAc(2)	1.5
[E].CDIPIGAGICASYQTQTNSPR.[A]	2× carbamidomethyl [C1; C10]; 1× NeuAc(1)Hex(2)HexNAc(2)	2.91
[E].CDIPIGAGICASYQTQTNSPR.[A]	2× carbamidomethyl [C1; C10]; 1× NeuAc(2)Hex(1)HexNAc(1)	0.79
[E].CDIPIGAGICASYQTQTNSPR.[A]	2× carbamidomethyl [C1; C10]; 1× NeuAc(1)Hex(1)HexNAc(1)	0.72
[E].CDIPIGAGICASYQTQTNSPR.[A]	2× carbamidomethyl [C1; C10]; 1× Hex(1)HexNAc(1)	<0.1
[E].CDIPIGAGICASYQTQTNSPR.[A]	2× carbamidomethyl [C1; C10]; 1× HexNAc(1)	1.34
[E].CDIPIGAGICASYQTQTNSPR.[A]	2× carbamidomethyl [C1; C10]	87.22
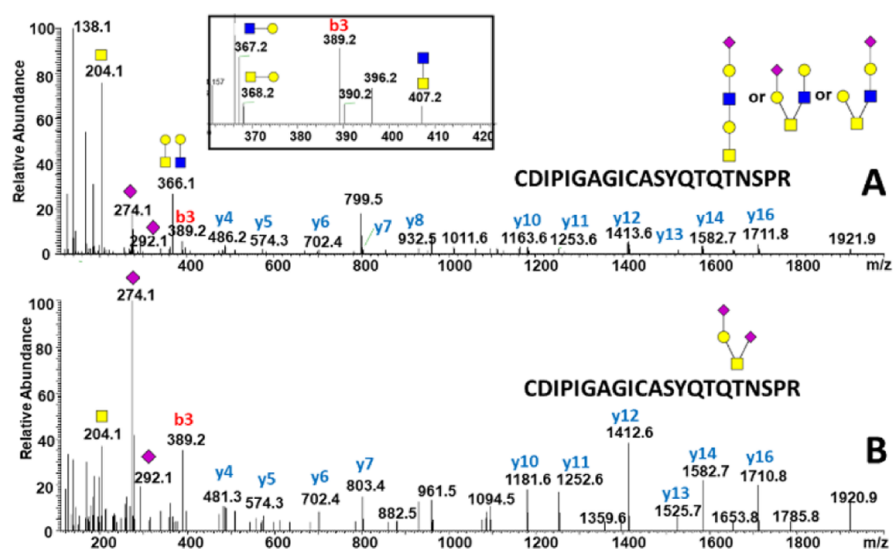
Figure 2. HCD tandem mass spectra of the SARS-CoV-2 S protein O-glycosylated on T678 with the following structures: (A) extended core-1 and core-2 structures and (B) disialylated core-1 structure. Inset: Oxonium ions in the HCD fragmentation spectrum confirm the presence of core-2 structures.
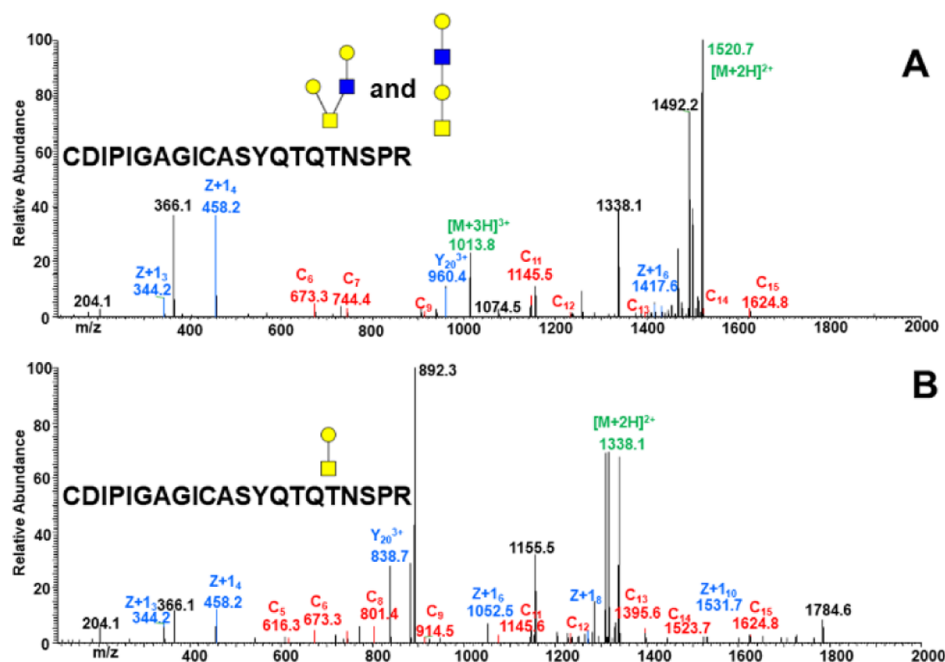

Figure 3. EThcD tandem mass spectra of a tryptic/GluC glycopeptide treated with PNGaseF and nonspecific neuraminidase confirming the occupancy of T678 by core-1 (B) and core-2 (A) structures.

galactosidases to resolve the HexNAc attachment on the O-glycopeptide even in the HCD spectra (Figure S3).

Structural Analysis of O-Glycopeptides Using Beam-Type Fragmentation. We chose cIMS[18] of oxonium ions to determine the structural features of O-glycopeptides of the SARS CoV-2 glycoprotein. We choose to use cIMS on the fragment to reduce the influence of the peptide backbone on the structural resolution. We were able to confirm the presence of core-2 structures by the diHexNAc fragment m/z 407 in the HCD spectra using the Orbitrap Fusion Lumos (Figure 2A inset). The tandem mass spectra obtained from the cIMS instrument preserve large oxonium ions, such as the intact detached glycan m/z 1022 (Figure 5), which confirms that a hexasaccharide occupies the O-glycopeptide AGC(cam)-

LIGAEHVNN(dea)SYEC(cam)DIPIGAGIC(cam)-ASYQTQTNSPR but using the beam-type fragmentation we could not determine which serine or threonine is occupied. We cannot fully exclude the possibility of contribution from a second glycan at this peptide, but neither the ETD not the HCD spectra show evidence of another occupied site besides the T678 of this peptide. We have also confirmed the presence of an extended core-1 structure associated with this glycopeptide by the fragments 528 and 819 observed in the spectra (Figure 5B).

Structural Analysis of O-Glycopeptides Using cIMS. We have used cIMS to separate isomeric oxonium ion fragments of the glycopeptides. We have used the m/z 657 ion to assign sialylation of the core-2 monosialylated structures.
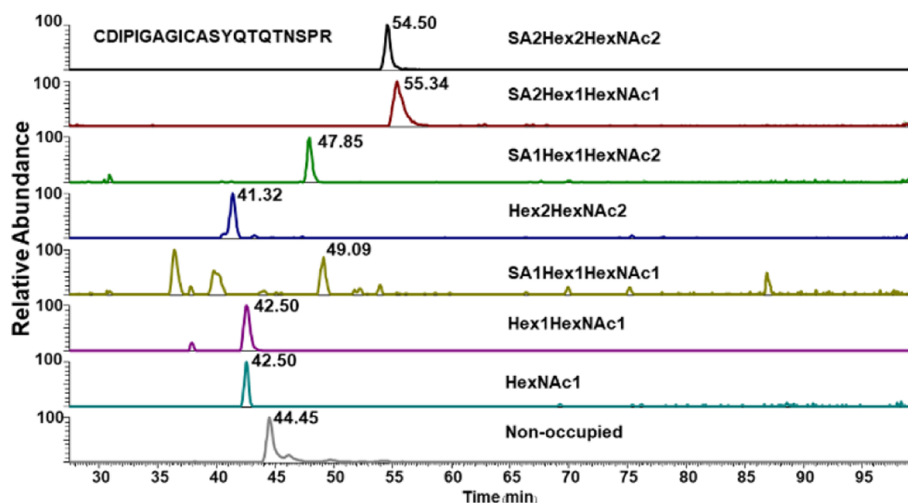
Figure 4. CDIPIGAGICASYQTQTNSPR O-glycopeptide of the SARS-CoV-2 S protein with the expected glycoform-dependent RT shifts visible in extracted ion chromatograms.
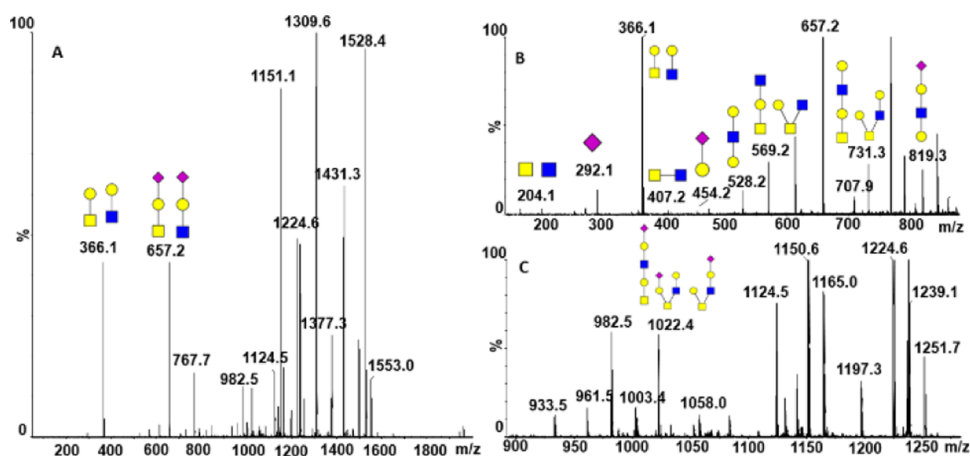

Figure 5. Beam-type tandem mass spectra of the AGC(cam)LIGAEHVNN(dea)SYEC(cam)DIPIGAGIC(cam)ASYQTQTNSPR (SA1Hex2-HexNAc2) O-glycopeptide with assigned extended core-1 and core-2 structures. The structures are characterized by the following fragments: (A) oxonium ions 366 and 657, generated from both core-1 and core-2 structures; (B) oxonium ion 407 specific for core-2 and ions 528 and 819 specific to the extended core-1 structure; and (C) oxonium ion 1022 corresponding to the detached intact glycans.

We used an optimized procedure based on a hemopexin glycopeptide standard, which we described previously,[12] and we determined CCS of fragment 657 (Figure 6) observed by fragmentation of the glycopeptide with a sialyl-T antigen with the linkage ($\alpha2-3$) (CCS 234.9) and by fragmentation of an N-glycopeptide with sialyl-LacNAc with ($\alpha2-6$) linkage (CCS 232.8) (data not shown).

This is in agreement with the previously published results on the linkages of the sialylated glycans.[6,8] We resolved two major IMS peaks in the cIMS of fragment m/z 657 using a one-pass method (Figure 7A). With five passes, the first peak was partially separated into two analytes with determined CCSs of 232.8 and 234.9 and a second peak CCS 248.5. This is reproducible for all 2HexNAc-containing structures (Figure S2). The CCS of the first peak fits exactly the previously observed CCS of sialylated $\alpha2-6$ LacNAc, while the CCS of the second peak fits the CCS of the sialylated $\alpha2-3$ T-antigen. CCS 248.5 of the third peak is in agreement with the previously described CCS of $\alpha2-3$ LacNAc.[19,20] The peak corresponding to the 2−6 linked sialic acid is better visible under high CE (Figure 7B−D) due to different stabilities of the Gal−SA bond.[21] We have determined a 7/3 ratio of SA-2-3-Gal-

GlcNAc and SA-2-3-Gal-GalNAc in the monosialylated core-2 structure (Figure 7, panel A). We used the cIMS of fragment m/z 731 (Hex 2HexNAc2) to determine the ratio of the core-2 structure and the extended core-1 structure. We obtained two major peaks using five passes of cIMS (data not shown); the first peak (time: 69.70; CCS: 238.8) is consistent with a core-2 structure and the second peak (76.84; CCS: 251.5) with a linear core-1 extended structure with terminal Gal(1−3)GalNAc, as described previously.[22] The ratio of core-1 with terminal Ga (1−3)GalNAc l and the core-2 structure is 25/75.

CONCLUSIONS

We have used our energy-optimized LC−MS/MS and ion mobility MS/MS methods to resolve structural motifs of N- and O-glycans of the SARS-CoV-2 S protein. We identified 17 N-glycopeptides, with many glycoforms including the LAcdiNAc and polyLacNAc structural motifs. This may not necessarily reflect the N-glycoforms of a virion, but the HEK293 expression system is commonly used for functional studies of the S-glycoprotein or the production of vaccine candidates, which means that resolution of the structures is
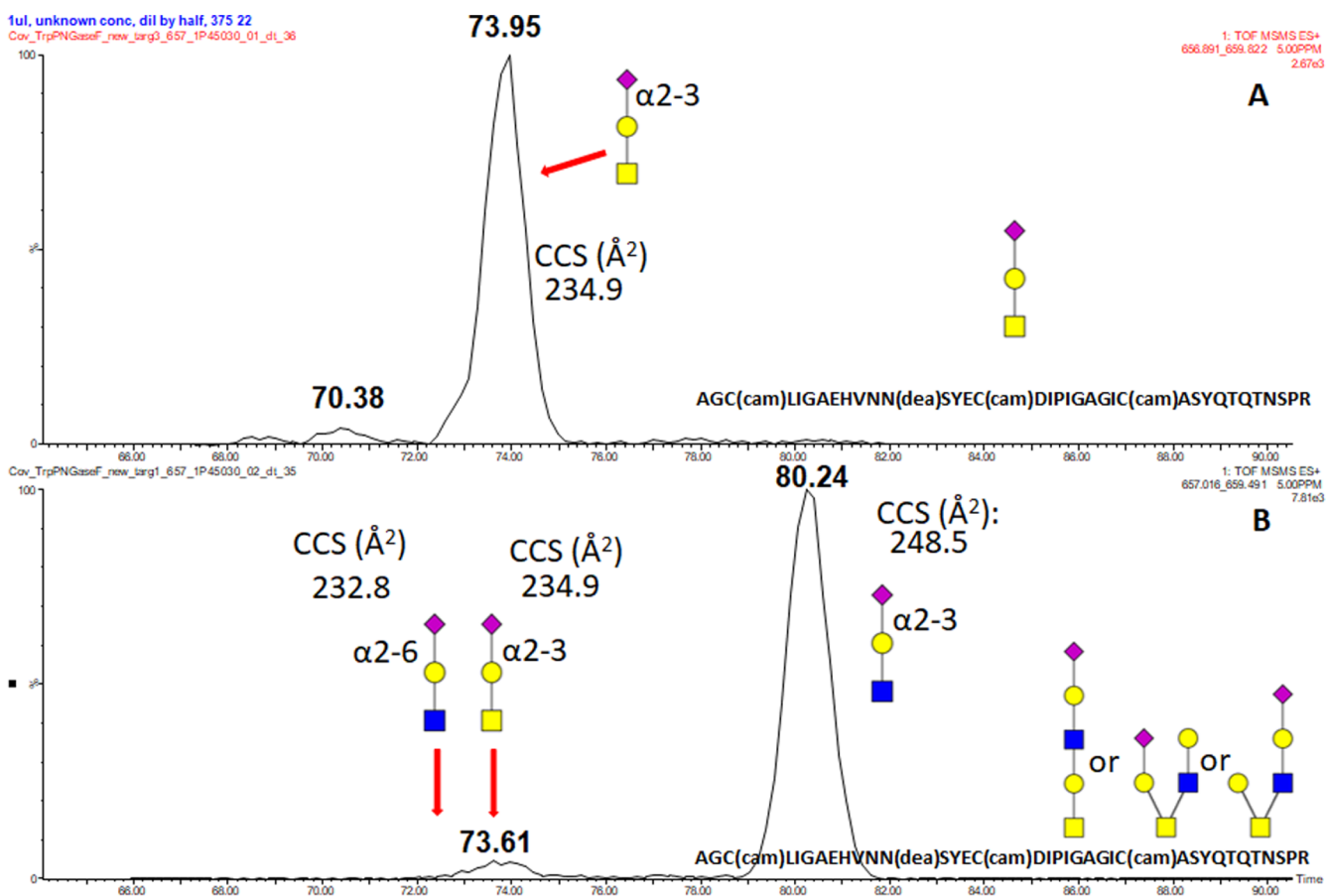
Figure 6. cIMS of fragment *m/z* 657 with measured CCS assignments produced by the fragmentation of AGC(cam)LIGAEHVNN(dea)SYEC-(cam)DIPIGAGIC(cam)ASYQTQTNSPR (SAHexHexNAc) (A) and (SAHex2HexNAc2) (B) O-glycopeptides produced by tryptic digests and PNGaseF deglycosylation of the SARS-CoV-2 S glycoprotein.
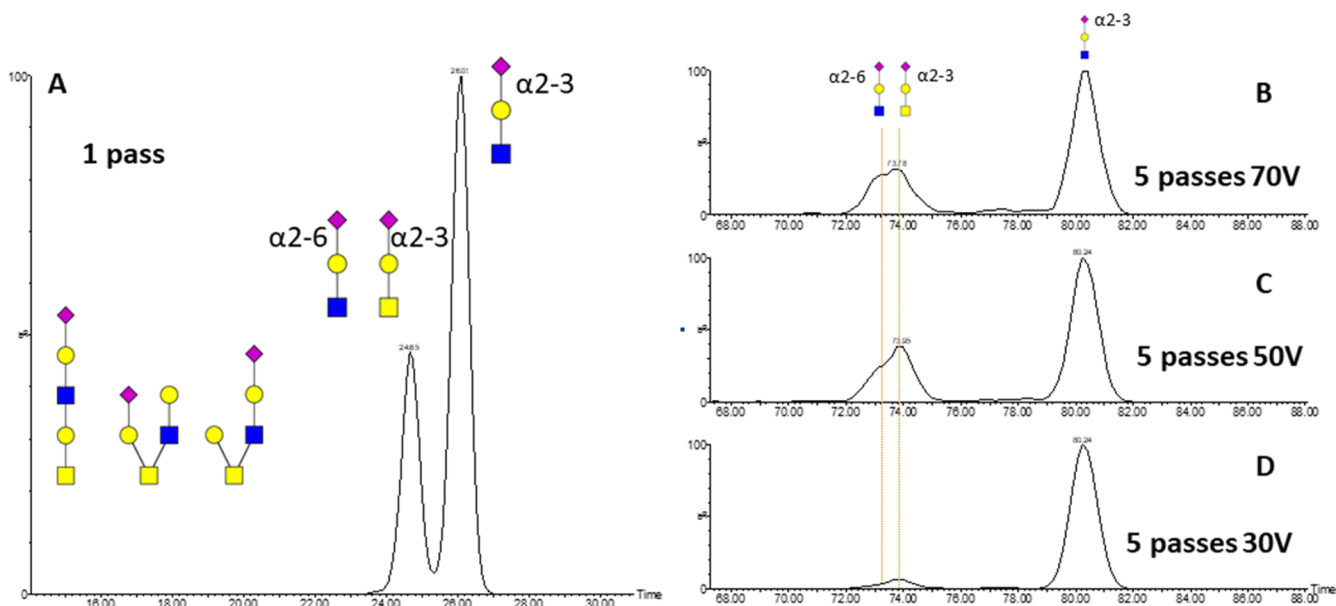

Figure 7. cIMS of the *m/z* 657 fragment produced by fragmentation of the AGC(cam)LIGAEHVNN(dea)SYEC(cam)DIPIGAGIC(cam)-ASYQTQTNSPR O-glycopeptide produced by tryptic digest and PNGaseF deglycosylation of the SARS-CoV-2 S glycoprotein using the following settings: (A) one-pass cIMS does not resolve SA (2−3) GalGalNAc and SA (2−6)GalGlcNAc; (B) five-pass cIMS with 70 V CE; (C) five-pass cIMS with 70 V CE; and (D) five-pass cIMS with 70 V CE. The ion mobilograms (B,C,D) show that multiple passes improve the resolution of isobaric [SA (2−3) GalGalNAc and SA (2−6) GalGlcNAc] structures and reveal the differences in the stability of sialic acid linkages.

highly relevant. Our findings are important for functional studies and the use of the protein as an immunization target. In addition, we identified, for the first time, an O-glycopeptide adjacent to the polybasic furin cleavage site located between the S1/S2 subunits that carry core-1 and core-2 structures capped primarily with $\alpha 2-3$ sialic acid at T678. The furin cleavage site is unique to the SARS-CoV-2 S protein compared to SARS-CoV of 2002, and its cleavage is potentially regulated by the nearby O-glycans as described for other convertases.[15] In addition, we identified eight additional O-glycopeptides of variable occupancy and unknown functional significance. The study substantially expands the knowledge of glycoforms of SARS-CoV-2 S expressed in the HEK293 cells and warrants further exploration of the impact of glycosylation on S-protein's function.

ASSOCIATED CONTENT

Supporting Information

The Supporting Information is available free of charge at https://pubs.acs.org/doi/10.1021/acs.analchem.0c03173.

MS2 spectra of YFKNHTSPDVD O-glycopeptide, cIMS analysis of 657 derived from different T678 O-glycopeptides, HCD spectra of Tn-antigen-occupied T678 O-glycopeptide, and certificate of analysis of SARS-Cov-2 S protein (R683A and R685A), His-tag (PDF)

Summary of SARS Cov2 spike glycoprotein glycosylation (XLSX)

Data are available in the following link: https://repository.jpostdb.org/preview/14997783515fb8a577b126f, access code: 6639.

AUTHOR INFORMATION

Corresponding Author

Miloslav Sanda − *Department of Oncology, Lombardi Comprehensive Cancer Center, Georgetown University, Washington, District of Columbia 20057, United States; Clinical and Translational Glycoscience Research Center, Georgetown University, Washington, District of Columbia 20057, United States;* orcid.org/0000-0002-7735-3635; Phone: +1 202-6876279; Email: ms2465@georgetown.edu; Fax: +1 202-6871988

Authors

Lindsay Morrison − *Waters Corporation Inc., Beverly, Massachusetts 01915, United States*

Radoslav Goldman − *Department of Oncology, Lombardi Comprehensive Cancer Center, Georgetown University, Washington, District of Columbia 20057, United States; Department of Biochemistry and Molecular & Cellular Biology and Clinical and Translational Glycoscience Research Center, Georgetown University, Washington, District of Columbia 20057, United States;* orcid.org/0000-0003-1304-0522

Complete contact information is available at:
https://pubs.acs.org/10.1021/acs.analchem.0c03173

Author Contributions

All the authors contributed to the writing of the manuscript and gave approval to the final version of the manuscript.

Notes

The authors declare no competing financial interest.

ACKNOWLEDGMENTS

REFERENCES

(1) *WHO Situation Report—71. Coronavirus Disease 2019 (COVID-19)*; WHO, 2020.

(2) Wu, F.; Zhao, S.; Yu, B.; Chen, Y. M.; Wang, W.; Song, Z. G.; Hu, Y.; Tao, Z. W.; Tian, J. H.; Pei, Y. Y.; Yuan, M. L.; Zhang, Y. L.; Dai, F. H.; Liu, Y.; Wang, Q. M.; Zheng, J. J.; Xu, L.; Holmes, E. C.; Zhang, Y. Z. *Nature* **2020**, *579*, 265−269.

(3) Wrapp, D.; Wang, N.; Corbett, K. S.; Goldsmith, J. A.; Hsieh, C.-L.; Abiona, O.; Graham, B. S.; McLellan, J. S. *Science* **2020**, *367*, 1260−1263.

(4) Jeffers, S. A.; Tusell, S. M.; Gillim-Ross, L.; Hemmila, E. M.; Achenbach, J. E.; Babcock, G. J.; Thomas, W. D.; Thackray, L. B.; Young, M. D.; Mason, R. J.; Ambrosino, D. M.; Wentworth, D. E.; DeMartini, J. C.; Holmes, K. V. *Proc. Natl. Acad. Sci. U.S.A.* **2004**, *101*, 15748−15753.

(5) Zou, X.; Moore, M. J.; Vasilieva, N.; Sui, J. H.; Wong, S. K.; Berne, M. A.; Somasundaran, M.; Sullivan, J. L.; Luzuriaga, K.; Greenough, T. C.; Choe, H.; Farzan, M. *Front. Med.* **2020**, *14*, 185−192.

(6) Watanabe, Y.; Allen, J. D.; Wrapp, D.; McLellan, J. S.; Crispin, M. *Science* **2020**, *369*, 330−333.

(7) Andersen, K. G.; Rambaut, A.; Lipkin, W. I.; Holmes, E. C.; Garry, R. F. *Nat. Med.* **2020**, *26*, 450−452.

(8) Shajahan, A.; Supekar, N. T.; Gleinich, A. S.; Azadi, P. *Glycobiology* **2020**, *30* (12), 981−988.

(9) Zhang, Y.; Zhao, W.; Mao, Y.; Wang, S.; Zhong, Y.; Su, T.; Gong, M.; Lu, X.; Cheng, J.; Yang, H. Site-Specific N-Glycosylation Characterization of Recombinant SARS-CoV-2 Spike Proteins Using High-Resolution Mass Spectrometry. *bioRxiv*, **2020**, arXiv:10.1101/2020.03.28.013276.

(10) Sanda, M.; Benicky, J.; Goldman, R. *Anal. Chem.* **2020**, *92*, 8262−8267.

(11) Pompach, P.; Brnakova, Z.; Sanda, M.; Wu, J.; Edwards, N.; Goldman, R. *Mol. Cell. Proteomics* **2013**, *12*, 1281−1293.

(12) Sanda, M.; Benicky, J.; Wu, J.; Wang, Y.; Makambi, K.; Ahn, J.; Smith, C. I.; Zhao, P.; Zhang, L.; Goldman, R. *Clin. Proteomics* **2016**, *13*, 24.

(13) Benicky, J.; Sanda, M.; Brnakova Kennedy, Z.; Goldman, R. *J. Biol. Chem.* **2019**, *294*, 16816−16830.

(14) Yuan, W.; Benicky, J.; Wei, R.; Goldman, R.; Sanda, M. *J. Proteome Res.* **2018**, *17*, 2755−2766.

(15) Schjoldager, K. T.; Vester-Christensen, M. B.; Goth, C. K.; Petersen, T. N.; Brunak, S.; Bennett, E. P.; Levery, S. B.; Clausen, H. *J. Biol. Chem.* **2011**, *286*, 40122−40132.

(16) Kozlik, P.; Goldman, R.; Sanda, M. *Electrophoresis* **2017**, *38*, 2193−2199.

(17) Kozlik, P.; Sanda, M.; Goldman, R. *J. Chromatogr. A* **2017**, *1519*, 152−155.

(18) Giles, K.; Ujma, J.; Wildgoose, J.; Pringle, S.; Richardson, K.; Langridge, D.; Green, M. *Anal. Chem.* **2019**, *91*, 8564−8573.

(19) Guttman, M.; Lee, K. K. *Anal. Chem.* **2016**, *88*, 5212−5217.

(20) Barroso, A.; Giménez, E.; Konijnenberg, A.; Sancho, J.; Sanz-Nebot, V.; Sobott, F. *J. Proteomics* **2018**, *173*, 22−31.

(21) Depraz Depland, A.; Renois-Predelus, G.; Schindler, B.; Compagnon, I. *Int. J. Mass Spectrom.* **2018**, *434*, 65−69.

(22) Jin, C.; Harvey, D. J.; Struwe, W. B.; Karlsson, N. G. *Anal. Chem.* **2019**, *91*, 10604−10613.